Permanent Magnets Synchronous Machines Faults Detection and Identification

Garance Vinson[1,2], Michel Combacau[2], Thomas Prado[1], Pauline Ribot[2]

1: Messier-Bugatti-Dowty, 78140 Velizy-Villacoublay, France

2: CNRS LAAS, 7 av du Colonel Roche, Univ de Toulouse, LAAS-UPS, 31400 Toulouse, France

Email: garance.vinson@safranmbd.com

Abstract—The reported work is the design of a Fault Detection system for permanent magnet synchronous machines (PMSM). Two main faults occurring on these machines are identified as inter-turns short-circuits and rotor single pole demagnetization, and characterized. An analytical model of the PMSM is developed and simulated using Matlab Simulink. The model enables simulating nominal and faulty PMSM behavior, with several stages of degradation, and is supported by tests results. Specific indicators are proposed for each fault. They do not require additional material or sensors since they are based on the signals already monitored for the machine control. An application is made on a 9-slots 8-poles synchronous machine being popular in aeronautics.

I. INTRODUCTION

Facing the growth of the air transport demand, the environmental issues and the competition between aircraft manufacturers, the aerospace industry is looking for safer, cleaner and cheaper aircrafts. Beside the major step changes occurring in engines, structures and aerodynamics, improvement of efficient secondary power systems offers promising advances. In this area, flight control and landing gears actuation appear as major power consumers that makes them a key driver for the sizing of the redundant aircraft power networks. As power is conveyed without mass transfer with electrical wires, power-by-wire has evident advantages against pneumatic or hydraulic power distribution.

The electrification of aeronautical systems is linked to another concern of Aircraft manufacturers. Indeed requirements are increasing regarding operational availability of equipment and a more efficient management of the maintenance. To achieve this, two families of solution can be combined: during design with the development of fault tolerant or fault resistant components, and during operational life with health monitoring. This latest appears as a very promising solution. However, implementing mature health monitoring features cannot be achieved without significantly improving the knowledge of the components wear and failures to enable proposing solutions for early fault detection, diagnosis and prognosis.

This paper specifically deals with FDI (fault detection and isolation). This process consists in (1) the detection of an abnormal behavior of the system under study and (2) the identification of the fault. This last task consists in identifying the faulty component and the fault gravity. It determines the health of the system and its components.

FDI's basic principle is to compare the real behavior of the system with the expected behavior that comes from a system model. Comparison is firstly made with the model of nominal operation during the detection stage. If there is a difference between observed and simulated nominal behaviours, then identification process takes place and comparison is done with other models representing faulty behaviours.

To assess the consistency between real and expected behaviours, indicators are used. These indicators are based on the information available on the system e.g. on the observations coming from the sensors. For each fault, a battery of indicators is used whose values vary in a well-known way when the fault occurs; this is the fault signature. This signature is identified from a model of the system including healthy and faulty behaviours. This model might be analytical, numerical, or both, depending on the knowledge available on the faulty system.

The reported work is the design of a FDI system for synchronous machines. An application is made on a 9-slots 8-poles synchronous machine used in safe critical aerospace actuation, e.g. for electrical brake. First the context of the study and the needs are described. Second the two main faults occurring on PMSM are identified and characterized. Third detection and diagnosis are discussed. Finally a conclusion summarizes the contribution and points out plans for future work.

II. PRESENTATION

A. The 9-slots 8-poles synchronous machine

In the domain of permanent magnet synchronous electrical machines, modular topology becomes more and more popular [1]. Teeth winding, also called concentrated winding, leads to very short end-winding improving the total axial length of the electrical machine. Compactness represents a significant advantage especially for small PMSM where the active stator pack is less than 100 mm. Moreover, these machines generate low torque ripple.

The studied machine is a 9-slots 8-poles 3-phases radial flux machine with non-overlapped coils and surface mounted permanent magnet. There are two coils a slot and they are wound in the sequence [A A A B B B C C C]. These machines are popular in aeronautics, they are meant to be used for other applications developed at Messier-Bugatti-Dowty. Their behavior is modelled as follows. Voltages induced into coils

by the rotor, E_a, E_b and Ec are a function of the rotor to stator mechanical position and of a parameter K_e depending on the coils configuration and number of turns and their model is described later. As coils are not surimposed, mutual inductances between phases are negligible and phase to phase voltage are:

$$U_{ab} = R(I_b - I_a) + L.d(I_b - I_a)/dt + E_b - E_a \quad (1)$$

$$U_{bc} = R(I_c - I_b) + L.d(I_c - I_b)/dt + E_c - E_b \quad (2)$$

$$I_a + I_b + I_c = 0 \quad (3)$$

where R and L are the phase resistance and inductance. Currents and induced voltages produce an electromagnetic torque C_{em} related to the PMSM mechanical speed Ω.

$$C_{em} = (E_a I_a + E_b I_b + E_c I_c)/\Omega \quad (4)$$

This PMSM being subject to faults, health monitoring is recquired and designed as explained in the next paragraph.

B. Health monitoring of the PMSM

PMSM can be advantageously monitored to enable just in time maintenance, that is to say planning the maintenance action right before the failure. In the reported work, a supervision system is designed. It consists in 2 modules: (1) a detection module warning when the machine does not operate properly, and (2) a diagnosis module isolating the fault.

Performing health monitoring requires wide knowledge of the system from the structural and functional point of view. This function/component mapping must be realized carefully and the interaction between components must be well-known. It is then common to perform a FMEA (Failure Mode Effects Analysis) to identify origins and consequences of the faults and to describe the degradation process.

The first step of the FDI system design is to choose which particular faults need to be monitored. For this purpose both frequency and gravity of all the possible machine faults are evaluated through in-service experience, tests, reliability analysis, and experts' judgement. Combining faults frequency and gravity allows assessing their criticality. Faults are then ranked with respect to criticality. Sudden faults are dismissed of the present study while only the progressive faults remain considered since they let time to develop a maintenance strategy before the machine fails.

Two faults are selected in this work. The most critical faults that are addressed here are inter-turns short-circuit and permanent magnet demagnetization. Next step is to characterize these faults to be able to detect, isolate, and as expected to prevent them.

III. INTER-TURNS SHORT-CIRCUITS

Winding turn's insulation is degraded by various causes like high temperatures variations and high voltage rates due to PWM (pulse width modulation) inverter fed. This insulation degradation comes finally to inter-turns short-circuits. Inter-turns short-circuits diminish the number of active turns in the affected phase, which then produces a smaller electromotive force. This leads to unbalanced statoric flux. It also creates a current loop, often called short-circuit loop. The current fluxing in this loop can be pretty high -up to 8 times the nominal current- leading to very high local temperatures and irreversible damages in the all system. For this reason, early detection of this fault is of particular importance since it may severely affect the machine performance or even destroy it.

Some authors as [2] perform FDI based on experimental results only. This can become very expensive if one wants the results for several degradation stages. In addition this approach cannot be generalized to other systems without any deeper theoretical study. That is why the author has chosen a model-based FDI.

A. Fault modelling

To gain knowledge on the machine behavior during inter-turns short-circuits, an analytical fault model is built. It is then simulated using Matlab Simulink as a time domain simulation tool. Insulation fault is represented with a variable resistor connecting two points of the coil as in [3], [4] and [5].
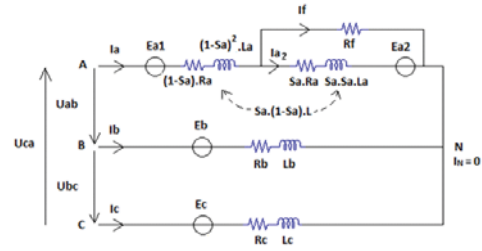

Fig. 1.   A-phase inter-turns short-circuit model

Two other parameters are involved, representing the fault severity. First, R_f represents the resistance of the turns insulator, that varies between 1000Ω typically for a healthy insulator and 0Ω for a direct short-circuit. Second, S_a represents the percentage of turns short-circuited in the $A-$phase. The model is represented in Figure 1, U_{ab}, U_{bc}, U_{ca} are the power supply voltages, E_{a1}, E_{a2}, E_b, E_c are the windings induced voltages, L_a, R_a, L_b, R_b, L_c, R_c are the phase inductances and resistances, I_a, I_b, I_c are the phase currents, I_f is the current fluxing in the short-circuit loop, $I_N = 0$ means that there is no neutral current and the sum of the three phase currents is nul.

The short-circuit loop equation gives:

$$I_f = I_a(S_a R + (S_a^2 L - M_a)j\omega)/(R_f + S_a R + S_a^2 Lj\omega) + E_a S_a/(R_f + S_a R + S_a^2 Lj\omega) \quad (5)$$

Equation (1) becomes:

$$U_{ab} = ZI_b + E_b - Z'_a I_a - (1 - S_a - Z_{ea})E_a \quad (6)$$

with

$$Z_{ea} = S_a(R_f + j\omega M_a)/(R_f + S_a R + S_a^2 Lj\omega) \quad (7)$$

and

$$Z_a' = (1 - S_a)R + j\omega(1 - S_a)^2 L - j\omega M_a + (R_f + j\omega M_a)(S_a R + (S_a^2 L - M_a)j\omega) / (R_f + S_a R + S_a^2 L j\omega) \quad (8)$$

A short-circuit indicator is then built from this model.

B. Inter-turns short-circuit indicator

The analytical study of the short-circuited electrical machine allows the author to build indicators based on sensors information. The author contribution is to base the indicator research on a deep analytical study instead of simulation or experimentation, which permits both a scientific reasoning and a generalization of the method whatever the application. Induced voltages and phase voltages have a $2\pi/3$ phase-shift. It is possible to express E_b and U_{bc} as: $E_b = E_a exp(j2\pi/3)$ and $U_{bc} = U_{ab}exp(j2\pi/3)$.

The relationship between phase currents can be expressed as: $I_b = X_b I_a$ and $I_c = X_c I_a$. In a healthy situation, the value of these coefficients are: $X_b = exp(j2\pi/3)$ and $X_c = exp(-j2\pi/3)$.

Induced voltages and phase to phase voltages are linked by the relations: $E_a = X_e U_{ab}, E_b = X_e U_{bc}$ and $E_c = X_e U_{ca}$, where X_e is a complex.

The author is looking for the relationship between I_b and I_a. To do so I_a is expressed as a function of U_{ab} in two different ways. Firstly, equation (6) gives $I_a = Z_2 U_{ab}$ with

$$Z_2 = (1 - (exp(j2\pi/3) - (1 - S_a - Z_{ea}))X_e) / (Z X_b - Z_a') \quad (9)$$

Secondly, equation (2) gives $I_a = Z_3 U_{ab}$ with

$$Z_3 = -(exp(j2\pi/3) + X_e + 2X_e.exp(j2\pi/3)) / (Z(1 + 2X_b))) \quad (10)$$

By solving $Z_2=Z_3$ the author finds X_b value which is the ratio between I_b and I_a:

$$X_b = (Z_a'exp((j2\pi)/3) - Z - ZX_e + Z_a'X_e + ZX_e exp((j2\pi)/3) + 2Z_a'X_e exp((j2\pi)/3) + S_a Z X_e - Z Z_{ea}X_e) / (2Z + Zexp((j2\pi)/3) + 3ZX_e - 2S_a Z X_e + 2Z Z_{ea}X_e) \quad (11)$$

The relationship between I_c and I_a is then deduced from equation (3) which gives $X_c = -1 - X_b$.

Another interesting relationship is the one between the faulty current I_a and the healthy current I_{anom}. In healthy conditions, $I_{anom} = Z_1 U_{ab}$ with

$$Z_1 = (1 - (exp(j2\pi/3) - 1)X_e)/(Z(exp(j2\pi/3) - 1)) \quad (12)$$

I_a/I_{anom} is then known from equations (9) and (12) and the analytical form is given by $I_a/I_{anom} = Z_2/Z_1$.

Finally, the short-circuited loop current I_f is compared to I_a. Indeed equation (5) leads to $I_f = X_f I_a$ with

$$X_f = (S_a R + (S_a^2 L - M_a)j\omega + S_a X_e/Z_2) / ((R_f + S_a R + S_a^2 L j\omega)) \quad (13)$$

All the currents I_b, I_c, I_f and I_{anom} are known from their relationship to I_a, and these relationships are a function of the short-circuit intensity characterized by R_f, S_a and other well known constant parameters. The evolution of phase and amplitude of I_a, I_b, I_f compared to I_a is shown in Figure 2.
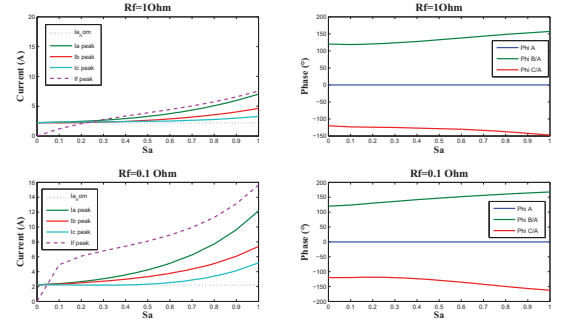

Fig. 2. Evolution of phases and magnitudes of currents as a function of Rf and Sa

Dynamic simulations are run with Matlab Simulink. Figure 3 shows the results of simulation of temporal evolution of phase currents.
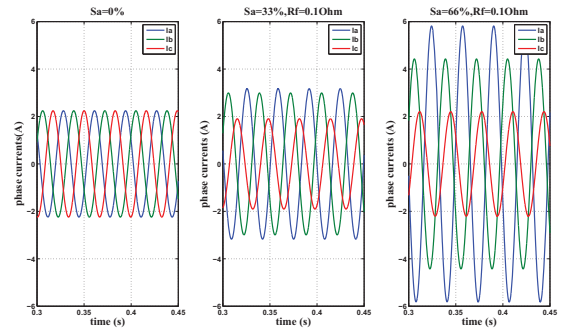

Fig. 3. Phase currents simulation results, with a healthy machine (left) and a A-phase partially short-circuited machine (right)

This simulation enhance the changes in phases and magnitudes of the three currents with the short-circuit, which can be well pointed out by the Fresnel diagram as in Figure 4. Graphically it is easy to deduce that the sum of the areas of the two triangles formed by faulty and nominal phase currents Ib and Ic is an efficient candidate for inter-turn short-circuit indicator. This area is computed as:

$$A_{sc} = |I_{bn}I_{bf}sin(\sigma_b)| + |I_{cn}I_{cf}sin(\sigma_c)|, \quad (14)$$

where I_n is the nominal current magnitude, I_f is the faulty current magnitude, and σ_b and σ_c are the angle between nominal ($\pm 2\pi/3$) and faulty phase shift between A-phase and
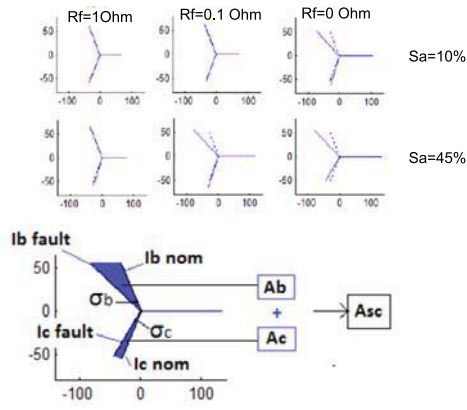
Fig. 4. Fresnel diagrams showing phases currents phase shift and magnitude changes for several values of Sa and Rf, and calculation of the Asc indicator

B or C-phase. The results of the calculations of this indicator for several short-circuit intensity are given in Figure 5.
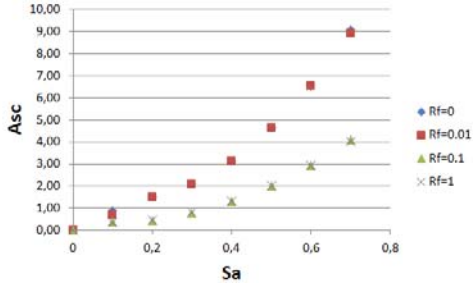

Fig. 5. Evolution of short-circuit indicator Asc for several values of Sa and Rf

The indicator can be computed on line from currents sensors thanks to currents phases and magnitudes. Its computed value corresponds to a certain degree of short-circuit characterized with R_f and S_a. This allows assessing the short-circuit gravity.

IV. PM DEMAGNETIZATION

The rotor also receives many stresses. High short-circuits currents, field weakening operation and high temperatures may demagnetize one or several poles of the rotor. This irreversibly decreases residual induction level of the magnets. One magnet may also be broken by centrifugal force or manufacturing default. Such a demagnetized pole creates a smaller induced voltage in the windings. This unbalances the rotor magnetic flux. Due to the machine symmetry, and opposite to the inter-turns short-circuit, the effect is the same on every phase. This difference with short-circuits will allow efficient discrimination between one fault and the other. This section presents the fault model and proposes a demagnetization indicator.

A. Fault modelling

1) Analytical model: The magnetic flux induced in a single coil is analytically modelled with the following hypotheses: no saturation, no magnetic leak in the magnetic circuit and uniform magnetic flux B_{max} induced by the magnet. A geometric analysis of the position of the magnet facing the coil leads to a fine approximation of the magnetic flux through the coil. The total flux through the three elementary coils of a phase is obtained by summation of their individual fluxes. It gives an analytical expression of the resulting piecewise-continuous function represented graphically in Figure 6 and 7. Taking the eight magnets into account, the flux in the three coils of a phase can be modeled. Its harmonic analysis shows
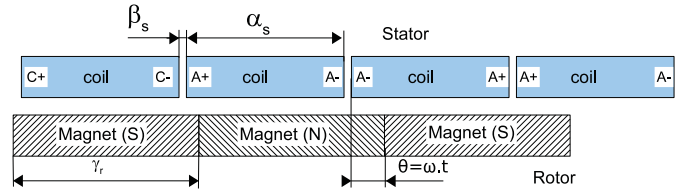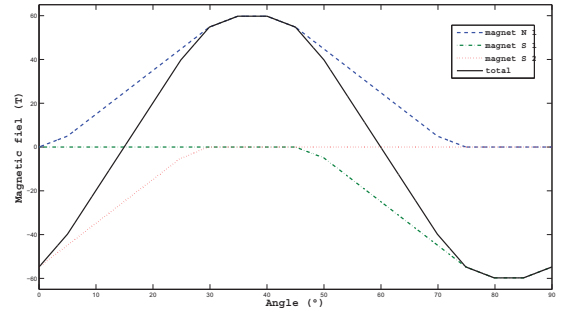

Fig. 6. Flux in the coils of a phase

Fig. 7. Repartition of the magnetical field created by the three magnets seen by one coil

these harmonics: H_4, H_{24} and H_{28} with $|H_4| = 20|H_{24}| = 25|H_{28}|$. The 4th harmonic carries more than 95% of the magnetic flux. The flux can be approximated by a sinusoidal function in healthy case.

To model the demagnetization, the author considers the flux from one of the magnets, which is diminished within the range $[0, B_{max}]$ to simulate a partial or total demagnetization.

2) Finite element model: To gain knowledge on the fault and to validate this simple analytical model a more precise model has been built (Figure 8). This temporal model is based on a steady-state model, developed using a design tool based on finite element calculation (FEMM). This FEMM model outputs the magnetic flux repartition and the induced voltages in case of demagnetization of the machine. Results are presented as a table giving induced voltage as a function of rotor position. Simulations are realized for 0, 25, 50, 75 and 100% of one single pole demagnetization. Computation step is 1.6 degree on a total of 360 degrees for a complete

rotor rotation, which means 225 points are computed for one turn.

The results are inserted into the dynamical model used to simulate the behavior of the engine in case of demagnetization. Induced voltages are replaced by three look-up tables. These look-up tables take electrical position and demagnetization percentage as inputs, and output induced voltage. Between the points computed with FEMM, values are linearly interpolated.
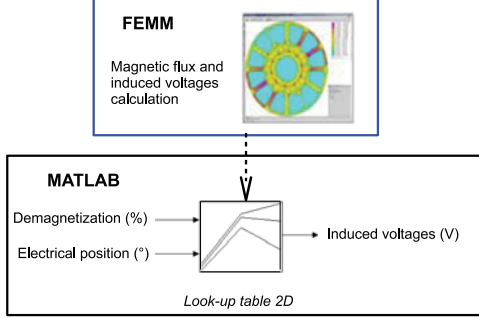

Fig. 8.   Demagnetization modelling method

This method allows combining the results precision of the finite element model and the high computing speed of the dynamic model. Results are presented for the 9-slots 8-poles machine, and the same method can be used for any PMSM. The modelling activities contribution is to enable simulating any numbers of poles instead of the two poles model often chosen for simplicity reason such as in [6].

B. Demagnetization indicator

The PMSM behavior is simulated for one single pole demagnetization between 0 and 100%. Temporal results are presented in Figure 9.
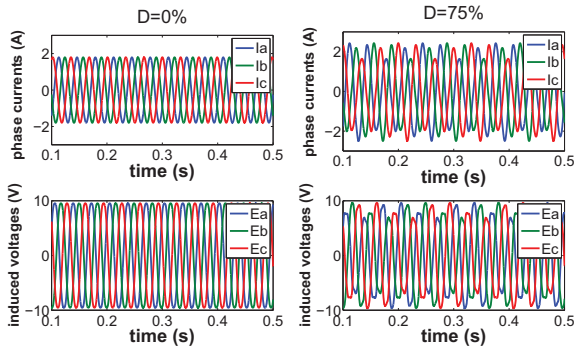

Fig. 9.   Temporal evolution of the phase currents in case of demagnetization of one pole

Obviously demagnetization leads to a different waveform for the induced voltages, which has repercussions on phase currents. A frequential analysis of these signals shows new harmonics appearings in these signals in case of one pole demagnetization. Results are shown in Table I.

Harmonic	1	2	4	5	13	14
Induced voltages	0.9%	2%	82%	12%	0.1%	3%
Phase currents	0%	0%	77%	11%	0%	3%

The energies of phase currents new harmonics are sum up to create the demagnetization indicator H_{dem}. For several simulation with different demagnetization percentage, H_{dem} is computed. The indicator evolution is shown in Figure 10.
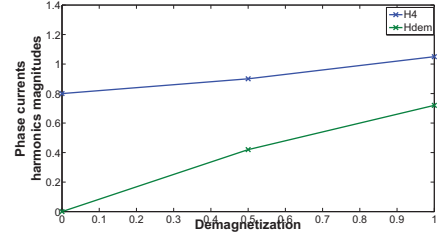

Fig. 10.   Evolution of phase currents fundamental harmonic H4 and of demagnetization indicator Hdem with one pole demagnetization.

H_{dem} increases progressively with the fault gravity, and can be evaluated on line thanks to currents sensors.

V. MODELS AND INDICATORS VALIDATION

A. Tests on faulted PMSM

In order to validate the model and the indicator choice, tests are run on short-circuited 9-slots 8-poles PMSM. Several PMSM with several unbalance degrees are tested and their short-circuit indicators A_{sc} are computed. Current measurements from tests are presented Figure 11.
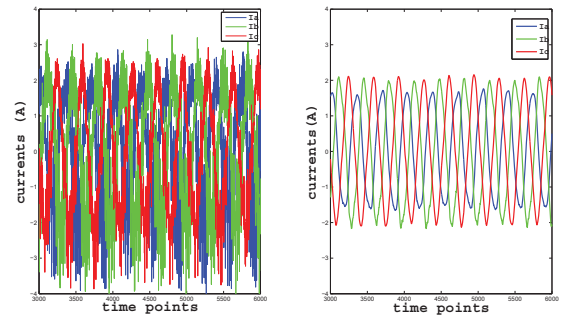

Fig. 11.   Test result for a short-circuited PMSM (Iunb=0.3). Sensors output (left) and filtered signals (right). Test configuration is: phase to phase voltage max is 22V, mechanical speed is 450 rpm, acquisition frequency is 10kHz.

The tested PMSM do not give access to the number of short-circuited turns S_a or to the short-circuit resistance R_f. On the other hand phases resistances depend on those two parameters and are measurable. The PMSM are therefore characterized by an unbalanced indicator I_{unb} calculated from

the phases resistances:

$$I_{unb} = \sqrt{\sum_{i=a,b,c} (R_i - R_{inom})^2} \qquad (15)$$

To compare tests and simulation results, I_{unb} is also computed for short-circuit models through the equation giving the model equivalent phase resistance as a function of the two model parameters R_f and S_a:

$$R_a = (1 - S_a)R_{anom} + S_a R_{anom} R_f / (S_a R_{anom} + R_f) \quad (16)$$

Comparison for the A_{sc} indicator value between tests and simulations is presented in Figure 12. Each test point represents a different PMSM.
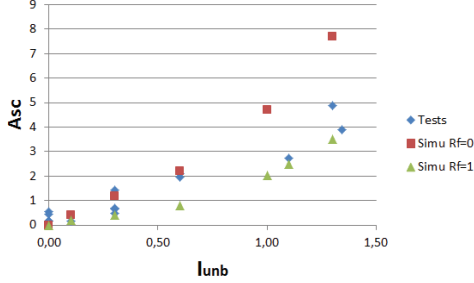

Fig. 12. Short-circuit indicator Asc variation as a function of unbalance indicator Iunb. Comparison between test and simulation results

Tests on short-circuited PMSM show results that are similar to those obtained with the short-circuit model. They are graphically in the area limited by the results obtained with $Rf = 0\Omega$ (direct short-circuit) and $Rf = 1\Omega$ (lighter short-circuit). The increase of Asc with the short-circuit gravity is clearly visible and progressive with the fault gravity.

Tests on demagnetized PMSM are in progress, first results are promising for the comparison between real PMSM and simulations.

B. Faults consequences comparison

In case of pole demagnetization without short-circuit A_{sc} remains equal to zero since there is no change in phase shift. This means that the proposed indicator is not affected by demagnetization, it is specific to inter-turns short-circuits. In case of short-circuit, H_{dem} remains equal to zero since the harmonics induced by inter-turns short-circuit are not the same. This indicator is specific to one pole partial or complete demagnetization. Consequences of the two faults are very different which allows easy discrimination between them.

It must be noticed that, in order to perform FDI, specific fault indicators have been built using only signals from phase currents and rotor vs stator angular position. These signals are available on airworthy PMSM. This is a great advantage for this kind of embedded application in term of cost and weight while others works [7] [8] design FDI systems with the help of electromagnetic flux sensors that is uneasy to implement on-board aircrafts. In case of currents sensors faults, the specific indicator would also be different. For instance there will be an offset, or the sum of the three currents would not be null. This can be considered as a perspective.

VI. CONCLUSION

The reported work is the design of a Fault Detection and Isolation system for synchronous machines. The two most critical faults occurring on this machine have been identified as inter-turns short-circuits and rotor pole demagnetization. Nominal and faulty models have been developed which simulation has provided a rich meant to identify the specific indicators for each fault. Unlike former studies that designed FDI systems with the resort to flux sensors that cannot be installed on- board, the proposed indicators only involve the available signals that are already used by the PMSM controller: phase currents and rotor vs stator position. An application is presented on a 9-slots 8-poles PMSM.

To continue this work the demagnetization analytical study will be detailed in order to define the indicator analytically. Tests on demagnetized PMSM are in progress and results will be compared with models results.

The natural extension of the FDI system is to study ageing laws of the PMSM and its components (such as insulator) in order to quantify the remaining time before failure and to optimize the maintenance schedule. In order to learn about short-circuit temporal evolution, some tests are in progress. The proposed supervision system will be completed with an additional module, the prognosis module, which aims to predict the future evolution of potential faults and the remaining useful life of our PMSM. The chosen faults are well adapted for prognosis since they are progressive, and since indicators values are increasing progressivly with faults severity.

REFERENCES

[1] F. Nierlich, "More electrical actuation for ata 32 : Modular power electronics and electrical motor concepts," in *SAE International*, 2010.
[2] A. J. M. Cardoso, S. M. A. Cruz, and D. S. B. Fonseca, "Inter-turn stator winding fault diagnosis in three-phase induction motors by park's vector approach," *IEEE Transactions on Energy Conversion*, vol. 14, no. 3, unknown 1999.
[3] M. Khov, "Monitoring of turn short-circuit faults in stator of pmsm in closed loop by on-line parameter estimation," Ph.D. dissertation, 2009.
[4] B. Vaseghi, "Modelling and study of pm machines with inter-turn fault dynamic model - fem model," *ELSEVIER, Electric Power Systems Research (EPSR)*, 2011.
[5] J.-C. Trigeassou, *Diagnostic des machines electriques*. Lavoisier, 2011.
[6] J. A. Farooq, A. Djerdir, and A. Miraoui, "7th ieee international symposium on diagnostics for electric machines, power electronics and drives," in *Proceedings of the 9th workshop on optimization and inverse problems in electromagnetism*, 2006.
[7] J. Penman, H. G. Sedding, and W. T. Fink, "Detection and location of interturn short circuits in the stator windings of operating motors," *IEEE Transactions on Energy Conversion*, vol. 9, no. 4, Jan 1994.
[8] D. Casadei, F. Filippetti, C. Rossi, and A. Stefani, "Magnet fault characterization for permanent magnet synchronous motors," in *IEEE International Symposium on diagnostics for Electric Machines, Power Electronics and Drives*, 2009.
[9] C. Ruschetti, G. Bossio, and C. D. Angelo, "Effects of partial rotor demagnetization on permanent magnet synchronous machines," in *IEEE International Conference on Industrial Technology (ICIT)*, 2010.